Title	Inhibition of prostate cancer cell growth by human secreted PDZ domain-containing protein 2, a potential autocrine prostate tumor suppressor
Author(s)	Tam, CW; Cheng, AS; Ma, RYM; Yao, KM; Shiu, SYW
Citation	Endocrinology, 2006, v. 147 n. 11, p. 5023-5033
Issued Date	2006
URL	http://hdl.handle.net/10722/54245
Rights	Endocrinology. Copyright © The Endocrine Society.

0013-7227/06/$15.00/0
Printed in U.S.A.

Endocrinology 147(11):0000–0000

doi: 10.1210/en.2006-0207

Inhibition of Prostate Cancer Cell Growth by Human Secreted PDZ Domain 2 Protein, a Potential Autocrine Prostate Tumor Suppressor

C. W. Tam, A. S. Cheng, R. Y. M. Ma, K.-M. Yao, and S. Y. W. Shiu

Departments of Physiology (C.W.T., A.S.C., S.Y.W.S.) and Biochemistry (R.Y.M.M., K.-M.Y.), The University of Hong Kong, Hong Kong, China

A possible role of the PDZ domain-containing protein 2 (PDZD2) in prostate tumorigenesis has been suggested. Besides, PDZD2 is posttranslationally cleaved by a caspase-dependent mechanism to form a secreted PDZ domain-containing protein 2 (sPDZD2) with unknown functions in humans. In this study, we demonstrate the endogenous expression of PDZD2 and secretion of sPDZD2 in cancerous DU145, PC-3, 22Rv1, LNCaP, and immortalized RWPE-1 prostate epithelial cells. Inhibition of endogenous sPDZD2 production and secretion by DU145, PC-3, 22Rv1, and RWPE-1 cells via the caspase-3 inhibitor Z-DEVD-FMK resulted in increased cell proliferation, which was abrogated by treatment with exogenous recombinant sPDZD2. Whereas sPDZD2-induced antiproliferation in DU145, PC-3, and 22Rv1 cells, it induced apoptosis in LNCaP cells. The data suggest that endogenous sPDZD2, produced by caspase-3-mediated cleavage from PDZD2, may function as a novel autocrine growth suppressor for human prostate cancer cells. The antiproliferative effect of sPDZD2 was apparently mediated through slowing the entry of DU145, PC-3, and 22Rv1 cells into the S phase of the cell cycle. In DU145 cells, this can be attributed to stimulated p53 and $p21^{CIP1/WAF1}$ expression by sPDZD2. On the other hand, the apoptotic effect of sPDZD2 on LNCaP cells was apparently mediated via p53-independent Bad stimulation. Together our results indicate the presence of p53-dependent and p53-independent PDZD2/sPDZD2 autocrine growth suppressive signaling pathways in human prostate cancer cells and suggest a novel therapeutic approach of harnessing the latent tumor-suppressive potential of an endogenous autocrine signaling protein like sPDZD2 to inhibit prostate cancer growth. (*Endocrinology* 147: 0000–0000, 2006)

GLOBALLY, PROSTATE CANCER has become the third most common cancer in men, with half a million new cases each year, amounting to about 10% of all male cancers (1). It is the most common cancer after skin cancer and is the second leading cause of cancer-related death in men in the United States. The emergence of prostate cancer as a public health problem in developed countries has put tremendous pressure on the health care system to provide new and effective treatments. Current understanding of cancer cell biology has allowed scientists to develop a rational approach to combat cancer cells by using a combination of anticancer drugs, which would inactivate and/or activate, respectively, multiple targets in cell growth-promoting and growth-inhibitory signaling pathways. Whereas there is significant research progress on understanding the signaling mechanisms of androgen, a key growth-promoting hormone, in prostate cancer initiation and progression, advanced prostate cancer patients still suffer from inevitable relapse of the disease after receiving the recommended treatment of androgen deprivation therapy (2). Besides androgen, various classical growth factors such as epidermal growth factor, IGF, and TGFβ have also been implicated, mostly, in the activation of prostate cancer growth (3, 4). Notwithstanding, therapeutic targets identified by these more classical growth-regulatory pathways are still in the process of successful translation into clinical use. Clearly there is an unmet clinical need to develop other novel therapeutic agents that can act effectively alone and/or in combination with androgen deprivation therapy to halt or reverse the progression of advanced prostate cancer. Such demand has fueled the search for novel endo-/para-/autocrine growth-promoting and growth-inhibitory signaling pathways important in prostate cancer pathogenesis, which may yield new therapeutic agents or targets for antiprostate cancer drug discovery and development. Of note, the recent success in the identification and inhibition of Hedgehog-Gli signaling pathways in prostate cancer growth has indeed opened up a new therapeutic strategy for prostate cancer (5–8).

PDZ domain-containing protein 2 (*PDZD2*) {also named *KIAA0300* (9), PIN-1 (10), PAPIN (11), activated in prostate cancer (*AIPC*) (12), and PDZ domain-containing protein 3 (*PDZK3*)}, is a six-PDZ (for PSD95, Discs-large, and ZO-1) domain protein, which is expressed in multiple tissues (13). Although proteins containing PDZ domains have been shown to bind specific C-terminal protein sequences of transmembrane receptors or ion channels and is believed to be involved in mediating intracellular protein-protein interactions, protein scaffolding, and intracellular signaling (14, 15), the functions of PDZD2 in humans are yet unknown. Interestingly, a possible role of PDZD2 (AIPC) in prostate cancer

First Published Online July 27, 2006

Abbreviations: AIPC, Activated in prostate cancer; BrdU, 5-bromo-2′-deoxyuridine; FBS, fetal bovine serum; MTS, 3-(4,5-dimethylthiazol-2-yl)-5-(3-carboxymethoxyphenyl)-2-(4-sulfophenyl)-2H-tetrazolium; PARP, poly(ADP-ribose) polymerase; PDZD2, PDZ domain-containing protein 2; SDS, sodium dodecyl sulfate; sPDZD2, secreted PDZD2.

***Endocrinology* is published monthly by The Endocrine Society (http://www.endo-society.org), the foremost professional society serving the endocrine community.**

balt3/zee-end/zee-end/zee01106/zee2979-06a | taylormp | S=6 | 8/23/06 | 20:40 | Art: EN-06-0207 | Input-ss

pathogenesis has recently been suggested by a significant increase in *PDZD2* (*AIPC*) gene and protein expression in prostate cancer tissues (12). Besides, the protein has also been shown to be posttranslationally cleaved by a caspase-dependent mechanism to form a secreted PDZ domain-containing protein 2 (sPDZD2) (13). Taken together, it would be of interest to determine whether sPDZD2, a posttranslationally cleavage product of PDZD2 (AIPC), may act as a novel autocrine signal important in prostate cancer pathogenesis. In this report, we studied the expression of sPDZD2 in human prostate cancer cells as well as the actions and mechanisms of sPDZD2 on prostate cancer cell growth modulation.

Materials and Methods

Human cancerous/immortalized cell lines and recombinant sPDZD2 synthesis

Human prostate cancer cell lines LNCaP.FGC (CRL-1740), DU145 (HTB-81), PC-3 (CRL-1435), and 22Rv1 (CRL-2505) as well as a human papillomavirus 18 transformed human prostate epithelial cell line RWPE-1 (CRL-11609) were obtained from American Type Culture Collection (Manassas, VA). LNCaP and 22Rv1 cells were propagated in RPMI 1640 medium (Life Technologies, Inc., Grand Island, NY) supplemented with L-glutamine and 10% fetal bovine serum (FBS) (Life Technologies), whereas DU145 and PC-3 cells were, respectively, propagated in Eagle's MEM (Life Technologies) and F-12 (Ham) (Life Technologies) medium supplemented with 10% FBS. RWPE-1 cells were cultured in keratinocyte-serum free medium supplemented with 50 μg/ml bovine pituitary extract and 5 ng/ml human recombinant epidermal growth factor (Life Technologies). All cell lines were incubated at 37 C with 5% CO_2 humidified atmosphere. Recombinant human sPDZD2 was synthesized and purified as previously described using the IMPACT (Intein Mediated Purification with an Affinity Chitin-binding Tag)-CN system (New England Biolabs, Beverly, MA) (16). AQ: A

Cell proliferation, viability, and apoptosis assays

DU145, PC-3, 22Rv1, and RWPE-1 cells (2×10^4/ml) were seeded in 96-well plates and incubated with or without 10^{-9}, 10^{-8}, and 10^{-7} M purified recombinant sPDZD2 or vehicle control [20 mM Tris-HCl (pH 8), 1 mM EDTA] for 24 and 48 h before the cells were processed for cell proliferation studies. In separate sets of experiments, DU145, PC-3, 22Rv1, and RWPE-1 cells were incubated with 10 μM specific caspase-3 peptide inhibitor, Z-DEVD-FMK (BD Biosciences, San Diego, CA), 10 μM-specific caspase-8 peptide inhibitor, Z-IETD-FMK (BD Biosciences), 10 μM negative control peptide Z-FA-FMK (BD Biosciences), or vehicle for 24 and 48 h. In addition, DU145, PC-3, 22Rv1, and RWPE-1 cells were each coincubated with 10 μM Z-DEVD-FMK and 10^{-8} M sPDZD2 for 48 h. Cell proliferation was measured by a tetrazolium-based Cell Titer 96 AQ_{ueous} assay kit (Promega, Madison, WI). Absorbance at 490 nm was recorded 3 h after 3-(4,5-dimethylthiazol-2-yl)-5-(3-carboxymethoxyphenyl)-2-(4-sulfophenyl)-2H-tetrazolium (MTS) addition. The proliferation of the cells was also monitored by a cell proliferation ELISA 5-bromo-2′-deoxyuridine (BrdU) (colorimetric) kit (Roche, Stockholm, Sweden), according to the manufacturer's protocol. Cell viabilities of LNCaP, DU145, PC-3, 22Rv1, and RWPE-1 cells, incubated with or without 10^{-9}, 10^{-8}, and 10^{-7} M purified recombinant sPDZD2 for 24 and 48 h, were measured by trypan blue dye exclusion assays. The number of viable cells was counted using hemocytometers. Any apoptotic effect on LNCaP cells induced by sPDZD2 was measured by the cell death detection $ELISA^{PLUS}$ assay kit (Roche), which detects the presence of mono- and oligonucleosomes in the cytoplasm of the cells after lysis. Briefly, LNCaP cells (1×10^5/ml) were seeded in 24-well plates and treated, under serum-free conditions, with or without 10^{-8} or 10^{-7} M sPDZD2, in the presence or absence of 10^{-9} M dihydrotestosterone for 24 h. After treatment, cells were harvested and any apoptosis was detected according to manufacturer's instructions. AQ: B AQ: C

Immunoblot analyses

For studies on the expression of PDZD2 and sPDZD2, PBS-washed native cancerous or immortalized prostate epithelial cells were incubated in their respective culture media without any added FBS for 24 h before the cells and conditioned media were collected for immunoblotting with the rabbit anti-PDZD2 antibody, which has been described previously (13). To study the effect of caspase inhibitors, the cells were incubated with or without 10 μM caspase-3 inhibitor Z-DEVD-FMK, 10 μM caspase-8 inhibitor Z-IETD-FMK, or 10 μM negative control peptide Z-FA-FMK under serum-free conditions for 48 h before immunoblotting analysis. For studies on the effects of sPDZD2 on the expression of proteins involved in cell cycle and apoptosis control, prostate cancer cells were harvested in lysis buffer [10 mM Tris-HCl (pH 7.4), 1% sodium dodecyl sulfate (SDS)] after they had been incubated with or without sPDZD2 for different time intervals. Lysates in sample buffer [0.2% SDS, 10% glycerol, 0.06 M Tris-HCl (pH 6.8), 100 mM dithiothreitol, and 0.01% bromophenol blue] were heated at 95 C for 5 min. Proteins in the conditioned media and recombinant sPDZD2 protein standards (10^{-12} to 10^{-7} M) were concentrated 50-fold using YM-10 Centricons (Millipore, Bedford, MA). Samples (10 μg) were resolved by SDS-PAGE and electroblotted to polyvinyl difluoride membranes (Millipore). The blots were blocked with 5% nonfat milk powder in TBS-T for 1 h at room temperature and then incubated with rabbit anti-PDZD2 antibody (1:10,000 dilution) overnight at 4 C. After washing with TBS-T, the blots were incubated with secondary antibodies against rabbit IgG (Zymed Laboratories, San Francisco, CA) and the signals were visualized by enhanced chemiluminescence Western blotting system (Amersham Biosciences, Piscataway, NJ). AQ: D AQ: E

To study the expression of $p21^{CIP1/WAF1}$, $p27^{KIP1}$, cyclin B, cyclin D, Bad, poly(ADP-ribose) polymerase (PARP), and p53 as well as the phosphorylation status of p53, the blots were incubated with primary antibodies against $p21^{CIP1/WAF1}$ (1:500 dilution, Santa Cruz Biotechnology, Santa Cruz, CA); $p27^{KIP1}$ (1:500 dilution; Santa Cruz Biotechnology); cyclin B (1:500 dilution; Santa Cruz Biotechnology); cyclin D (1:500 dilution; Santa Cruz Biotechnology); Bad (1:500 dilution; Santa Cruz Biotechnology); PARP (1:500 dilution; Santa Cruz Biotechnology); p53 (1:500 dilution; Santa Cruz Biotechnology); or primary phospho-p53 antibodies against Ser6, Ser9, Ser15, Ser20, Ser37, Ser46, and Ser392 phosphorylation sites (1:1000 dilution; Cell Signaling Technology, Beverly, MA) overnight at 4 C. After washing with TBS-T, the blots were incubated with secondary antibodies against mouse IgG (Amersham Biosciences) for $p21^{CIP1/WAF1}$, $p27^{KIP1}$, cyclin B, cyclin D, Bad, PARP, and p53 antibodies or secondary antibodies against rabbit IgG (Zymed Laboratories) for phospho-p53 antibodies. Blots were stripped in 25 mM glycine buffer (pH 2.0) for 30 min for reprobing with α-tubulin (1:500 dilution; Santa Cruz Biotechnology). The signals were visualized by enhanced chemiluminescence Western blotting system (Amersham Biosciences), and densitometric analyses of the developed blot normalized against α-tubulin were performed.

Transient reporter assay

DU145 cells (5×10^4/ml) were seeded onto 24-well plates. After 24 h, the cells were transiently transfected with Fugene 6 reagent (Roche). To each well, a mixture of 0.6 μl Fugene 6, 0.2 μg $p21^{CIP1/WAF1}$ reporter construct pGL3-p21pro or $p27^{KIP1}$ reporter construct pGL3-p27pro, and 0.04 μg *Renilla* luciferase reporter pRL-tk (Promega) were added. sPDZD2 (10^{-9}, 10^{-8}, and 10^{-7} M) or vehicle was added directly to the medium at one tenth dilution 24 h after transfection. After 24 and 48 h of incubation, Dual-Luciferase reporter assay system (Promega) was used to measure both the firefly and *Renilla* luciferase activities, according to the manufacturer's instructions. Briefly, the cells were washed thrice with PBS. Passive lysis buffer was added to each well and was shaken at room temperature for 15 min. Lysate (20 μl) from each sample was transferred to a 96-well plate for firefly and *Renilla* luciferase activity measurement by the microplate luminometer LB96V (EG&G Berthold, Bad Wildbad, Germany). AQ: F

RNA preparation and semiquantitative RT-PCR analyses

Total RNA was extracted from DU145 cells treated with or without 10^{-9}, 10^{-8}, and 10^{-7} M sPDZD2 for 24 h using TRIzol (Invitrogen,

balt3/zee-end/zee-end/zee01106/zee2979-06a | taylormp | S=6 | 8/23/06 | 20:40 | Art: EN-06-0207 | Input-ss

Carlsbad, CA), and the RNA (500 ng) was then reversely transcribed into cDNA by the SuperScript III first-strand synthesis system (Invitrogen) following the manufacturer's instructions. $p21^{CIP1/WAF1}$ cDNA was amplified by PCR using specific forward primer 5′-GCGATGGAACTTCGACTTTGT-3′ and reverse primer 5′-GGGCTTCCTCTTGGAGAAGAT-3′ designed from published $p21^{CIP1/WAF1}$ cDNA sequence as reported previously (17). Similarly, $p27^{KIP1}$ cDNA was amplified by PCR using specific forward primer 5′-CCACGAAGAGTTAACCCGGG-3′ and reverse primer 5′-GTCTGCTCCACAGAACCGGC-3′ designed from published $p27^{KIP1}$ cDNA sequence as described previously (18). Glyceraldehyde-3-phosphate dehydrogenase cDNA was amplified by PCR using specific forward primer 5′-GCAGGGGGAGCCAAAAGGG-3′ and reverse primer 5′-TGCCAGCCCCAGCGTCAAAG-3′. cDNA amounts and cycle numbers were optimized to ensure that amplification was within the linear range for quantitative analysis. The PCRs contained 2 μl cDNA, 1 pmol/μl primers, 1 mM deoxynucleotide triphosphate, 1× PCR buffer, 5 mM $MgCl_2$, and 1 U *Taq* DNA polymerase. The 40 cycles of PCR amplification were preceded by denaturation at 94 C for 2 min. Each PCR cycle consisted of denaturation at 94 C for 15 sec, annealing at 55 C for 30 sec, and extension at 70 C for 1 min. After the reaction, 10 μl of the PCR products were separated on an agarose gel [1.5% (wt/vol)]. The amplified $p21^{CIP1/WAF1}$ and $p27^{KIP1}$ cDNAs, normalized against *glyceraldehyde-3-phosphate dehydrogenase* cDNA in the same preparations, were quantitated.

Flow cytometry

Exponentially growing cells DU145, PC-3, and 22Rv1 were seeded in 25-cm^2 flasks at approximately 90% confluency. Cells were maintained at full confluency for 72 h to synchronize cells at early G_1. Cells were then released into cell cycle progression by replating onto new 25-cm^2 flasks, at approximately 30% confluency, in respective cell culture media with or without 10^{-8} M sPDZD2. The cells were harvested at specific time points, fixed in ethanol (70%,vol/vol) overnight, and treated with RNase (10 mg/ml). Propidium iodide (250 μg/ml) was then added to the samples, mixed, and incubated in the dark for at least 15 min. Flow cytometry was performed using the EPICS Elite ESP high-performance cell sorter (Coulter Electronics, Miami, FL). In separate sets of experiments, unsynchronized DU145, PC-3, and 22Rv1 cells were treated with the caspase-3 inhibitor Z-DEVD-FMK (10 μM) or the negative control peptide Z-FA-FMK (10 μM) for 24 and 48 h. The cells were then harvested as described above for DNA analyses. The raw data collected were analyzed by Modfit LT (version 2.0; Verity Software, Topsham, ME) to eliminate aggregated cells for determination of cell cycle distribution.

Statistical and data analysis

The data were analyzed with one-way ANOVA followed by Tukey's test. Two group comparisons were analyzed by unpaired Student's *t* test. The level of significance for all statistical analyses was set at $P < 0.05$.

Results

Endogenous PDZD2 expression and sPDZD2 secretion in cancerous and immortalized prostate epithelial cells

Chaib *et al.* (12) reported up-regulation of the full-length PDZD2 protein in prostate cancer, but expression of the secreted form of PDZD2, sPDZD2, has not been similarly studied. Using a specific anti-PDZD2 antiserum that recognize both the full-length and secreted forms of PDZD2 (13), we analyzed the lysates and conditioned media from cultured LNCaP, DU145, PC-3, 22Rv1, and RWPE-1 cells by immunoblotting. Full-length PDZD2 (301 kDa) and sPDZD2 (37 kDa) were detected, respectively, in the cell lysates and conditioned media of all the prostate cell lines (Fig. 1A). The lack of sPDZD2 expression in the cell lysates suggests that sPDZD2 is predominantly secreted rather than stored intracellularly after its cleavage from PDZD2.

Effects of caspase inhibitors on endogenous PDZD2 expression and sPDZD2 secretion and cell growth

Full-length PDZD2 protein, which exhibits close sequence homology to pro-IL-16, is processed and cleaved by a caspase-dependent mechanism to generate sPDZD2 (13). In light of the fact that cleavage of pro-IL-16 to form the corresponding secretory IL-16 cytokine is mediated by caspase-3 (19), it would be of interest to determine whether the proteolytic cleavage of full-length PDZD2 to its secreted protein sPDZD2 is caspase-3 dependent. DU145, PC-3, 22Rv1, and RWPE-1 cells were incubated for 48 h with 10 μM Z-DEVD-FMK (a specific inhibitor of caspase-3), 10 μM Z-IETD-FMK (a specific inhibitor of caspase-8), or 10 μM Z-FA-FMK (a negative control peptide). Treatment of DU145, PC-3, 22Rv1, and RWPE-1 cells with Z-DEVD-FMK for 48 h resulted in 40, 28, 44, and 50% reduction of sPDZD2 secretion into the respective conditioned media, compared with cells treated with Z-FA-FMK (Fig. 1B). Concomitantly, PDZD2 expression in DU145, PC-3, 22Rv1, and RWPE-1 cells showed respective 3-, 2-, 4.4-, and 3.7-fold increases, compared with Z-FA-FMK-treated cells (Fig. 1C). However, there were no changes in sPDZD2 secretion and PDZD2 expression after the cells were treated with the specific caspase-8 inhibitor Z-IETD-FMK (10 μM) for 48 h (data not shown). These data indicated that the proteolytic cleavage of PDZD2 is mediated by caspase-3.

To determine whether alterations in PDZD2 and sPDZD2 levels in inhibitor-treated cells are associated with any changes in the cell growth rate, we also monitored DU145, PC-3, 22Rv1, and RWPE-1 cell proliferation by MTS-based assays. Interestingly, there were significant ($P < 0.01$) increases in DU145 (20.1–22.7%), PC-3 (22.9–24.8%), 22Rv1 (23.4–26%), and RWPE-1 (20.9–24.2%) cell proliferation after the cells were treated with the caspase-3 inhibitor Z-DEVD-FMK (10 μM) for 24 and 48 h (Fig. 1, D–G). No changes in the proportion of cells in different cell-cycle phases were detected after treatment with the caspase-3 inhibitor for 24 and 48 h (data not shown). There were also no changes in the proliferation of the cells after 24 and 48 h treatment of 10 μM caspase-8 inhibitor Z-IETD-FMK (data not shown). To further examine whether the observed increases in cell proliferation were due to inhibition of sPDZD2 secretion, we tested the ability of exogenously applied recombinant sPDZD2 (16) to counteract the growth-promoting effects of the caspase-3 inhibitor. As shown in Fig. 1H, the increases in DU145, PC-3, 22Rv1, and RWPE-1 cell proliferation induced by caspase-3 inhibitor treatment were abolished by coincubating with 10^{-8} M sPDZD2. These results suggest that the antiproliferative effects were predominantly mediated by sPDZD2 instead of PDZD2.

Effects of recombinant sPDZD2 on cancerous and immortalized prostate epithelial cell growth

Recombinant sPDZD2 induced a significant ($P < 0.001$) concentration-dependent inhibition of cell proliferation in DU145, PC-3, and 22Rv1 cells (Fig. 2). No significant changes in RWPE-1 cell proliferation in response to recombinant sPDZD2 were observed (data not shown). Treatment of DU145 cells with 10^{-8} and 10^{-7} M sPDZD2 for 24 h resulted

balt3/zee-end/zee-end/zee01106/zee2979-06a | taylormp | S=6 | 8/23/06 | 20:40 | Art: EN-06-0207 | Input-ss

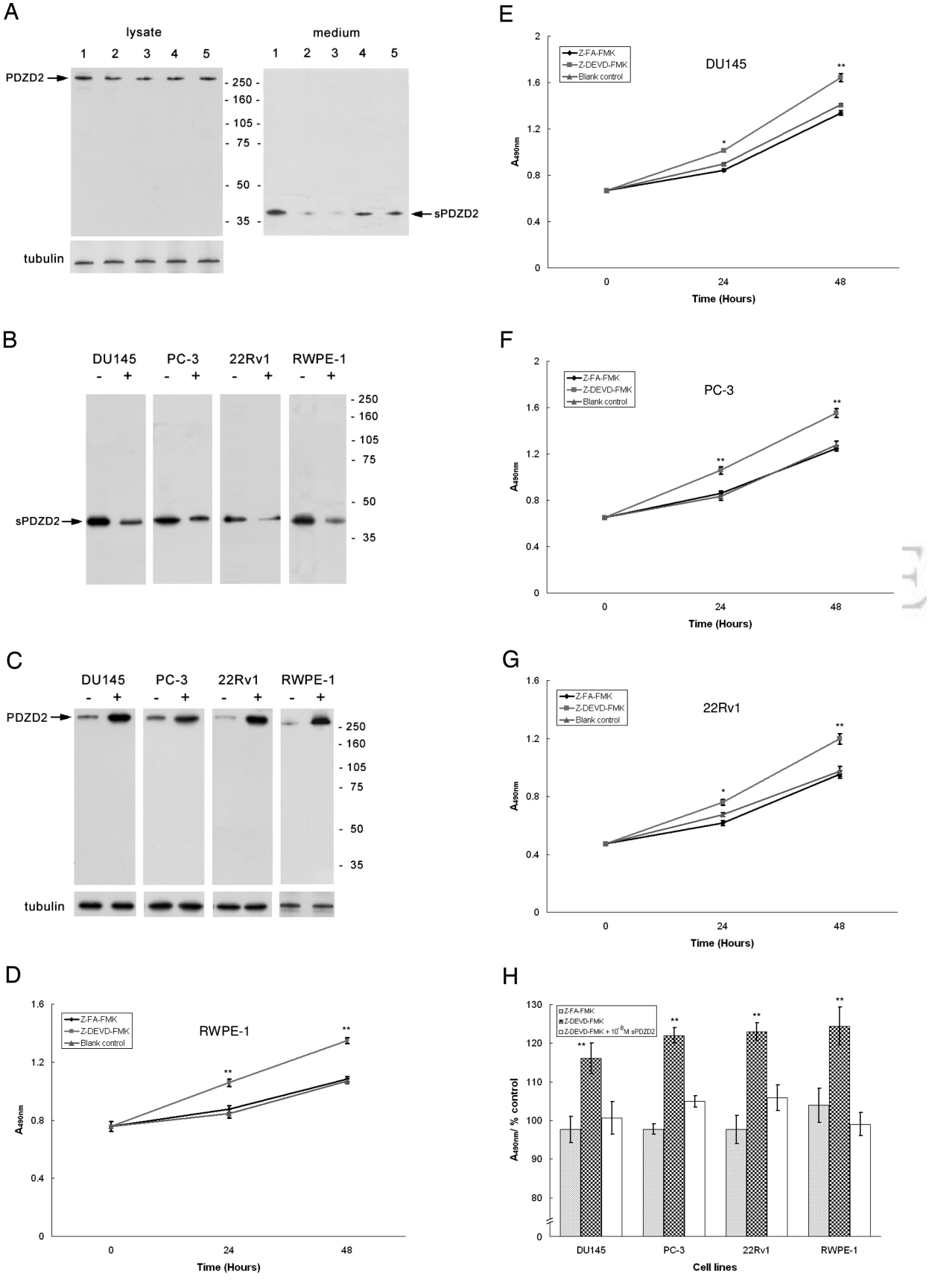

balt3/zee-end/zee-end/zee01106/zee2979-06a | taylormp | S=6 | 8/23/06 | 20:40 | Art: EN-06-0207 | Input-ss

in, respectively, 25.8 and 29.9% decreases in cell proliferation ($P < 0.001$). Treatment of PC-3 cells with 10^{-8} and 10^{-7} M sPDZD2 for 24 h resulted in, respectively, 13.5 and 22.6% decreases in cell proliferation ($P < 0.01$). Treatment of 22Rv1 cells with 10^{-8} and 10^{-7} M sPDZD2 for 24 h resulted in, respectively, 12.7 and 15.4% decreases in cell proliferation ($P < 0.001$). On the other hand, DU145 cell proliferation exhibited 38.6 and 43.5% decreases ($P < 0.001$) after the cells were treated with 10^{-8} and 10^{-7} M sPDZD2, respectively, for 48 h. PC-3 cell proliferation exhibited 23.8 and 41.6% decreases ($P < 0.001$) after the cells were treated with 10^{-8} and 10^{-7} M sPDZD2, respectively, for 48 h. 22Rv1 cell proliferation exhibited 21.7 and 27.7% decreases ($P < 0.001$) after the cells were treated with 10^{-8} and 10^{-7} M sPDZD2, respectively, for 48 h (Fig. 2, A–C). Similar antiproliferative effects of sPDZD2 on DU145, PC-3, and 22Rv1 cells were also demonstrated using the Cell Proliferation ELISA BrdU (colorimetric) kit (Roche) (Fig. 2, D–F). No changes in DU145, PC-3, 22Rv1, and RWPE-1 cell viabilities were detected (data not shown).

Effects of sPDZD2 on regulation of proteins involved in cell cycle control

Given that sPDZD2 induced the strongest antiproliferative effects on DU145 cells, compared with PC-3 and 22Rv1 cells (Fig. 2), we selected DU145 as the principal prostate cancer cell model to explore the intracellular mechanisms that may mediate the growth-inhibitory effects of sPDZD2. DU145 cells were treated with 10^{-9}, 10^{-8}, and 10^{-7} M sPDZD2 for 48 h, and any sPDZD2-induced changes in the expression levels of $p21^{CIP1/WAF1}$, $p27^{KIP1}$, p53, cyclin B, and cyclin D were monitored. As shown in Fig. 3A, treatment of DU145 cells with 10^{-9}, 10^{-8}, and 10^{-7} M sPDZD2 for 48 h did not result in any changes in the level of $p27^{KIP1}$. No changes in the expression of cyclin B and cyclin D were also observed (data not shown). However, sPDZD2 induced changes in $p21^{CIP1/WAF1}$ and p53 in growth-inhibited DU145 cells (Fig. 3A). Treatment of DU145 cells with 10^{-8} and 10^{-7} M sPDZD2 for 48 h resulted in 4.5- and 4.4-fold increases in $p21^{CIP1/WAF1}$, respectively. In correlation, DU145 cells treated with 10^{-8} and 10^{-7} M sPDZD2 for 48 h, respectively, exhibited 3.9- and 3.8-fold increases in p53 expression. Of note, increased p53 expression (1.4-fold) was detected in DU145 cells after the cells had been incubated with 10^{-8} M sPDZD2 for 12 h. Relative to p53, the rise (2.6-fold) of $p21^{CIP1/WAF1}$ expression was delayed by 12 h in DU145 cells treated with 10^{-8} M sPDZD2 (Fig. 3B). To further elucidate the signaling mechanisms of sPDZD2 in DU145 cells, the phosphorylation status of p53 in response to sPDZD2 treatment was investigated. No significant changes in the phosphorylation status of p53 at Ser6, Ser9, Ser15, Ser20, Ser37, Ser46, and Ser392 phosphorylation sites were detected in DU145 treated with 10^{-8} and 10^{-7} M sPDZD2 for 1, 4, and 8 h (data not shown). On the other hand, no significant changes in $p21^{CIP1/WAF1}$, $p27^{KIP1}$, cyclin B, and cyclin D expression were observed in PC-3 cells, which showed no p53 expression (data not shown). Similarly, no significant changes in $p21^{CIP1/WAF1}$, $p27^{KIP1}$, p53, cyclin B, and cyclin D expression were observed in 22Rv1 cells (data not shown).

Apoptotic effects of sPDZD2 on LNCaP cells

Recombinant sPDZD2 did not induce any changes in the viabilities of DU145, PC-3, 22Rv1, and RWPE-1 cells. However, incubation of LNCaP cells with 10^{-7} M sPDZD2 for 24 h resulted in 26.2% decrease in cell viability ($P < 0.001$), whereas LNCaP cell viability exhibited 14.7 and 18.6% decreases ($P < 0.001$) after treatment with 10^{-8} and 10^{-7} M sPDZD2, respectively, for 48 h (Fig. 4A). The observed decreases in LNCaP cell viability in response to sPDZD2 were found to be due to apoptosis induction (Fig. 4B), as measured by cell death detection $ELISA^{PLUS}$ assay kit (Roche). Significant ($P < 0.001$) increases in absorbance at 405 nm, which reflects an increase in mono- and oligonucleosomes in the cell cytoplasm, were observed in LNCaP cells treated with 10^{-8} and 10^{-7} M sPDZD2 for 24 h. Because p53 is also a key regulator of apoptosis besides cell cycle progression (20), we also monitored the expression of p53 and the phosphorylation status of p53 at Ser15, Ser20, Ser37, and Ser46 phosphorylation sites, which are important in apoptosis control (21), in LNCaP cells. Treatment of the cells with 10^{-8} and 10^{-7} M sPDZD2 for 1, 2, and 4 h did not induce any changes in p53 levels and in its phosphorylation status at Ser15, Ser20, Ser37, and Ser46 (data not shown). Interestingly, treatment of LNCaP cells with 10^{-8} and 10^{-7} M sPDZD2 for 24 h resulted in respective 3.7- and 3.1-fold up-regulation in Bad expression. In addition, treatment of LNCaP cells with 10^{-8} and 10^{-7} M sPDZD2 for 48 h increased the expression of Bad by 2.6- and 2.1-fold, respectively (Fig. 4C). The cleavage of PARP, which serves as an early specific marker of apoptosis, was also observed after treatment of LNCaP cells with 10^{-8} and 10^{-7} M sPDZD2 for 24 and 48 h (Fig. 4C). In the presence of 10^{-9} M dihydrotestosterone, the apoptotic effects induced by 10^{-8} and 10^{-7} M sPDZD2 were significantly reduced (data not shown), indicating that androgen may confer protection against sPDZD2-induced apoptosis in LNCaP cells.

Effects of sPDZD2 on $p21^{CIP1/WAF1}$ and $p27^{KIP1}$ transcription

To determine whether the elevated $p21^{CIP1/WAF1}$ protein expression was caused by an increase in *$p21^{CIP1/WAF1}$* gene tran-

FIG. 1. Expression and secretion of PDZD2/sPDZD2 in cancerous and immortalized prostate epithelial cells and the effects of caspase-3 inhibitor Z-DEVD-FMK on PDZD2/sPDZD2 expression and secretion and cell growth. A, The presence of PDZD2 and sPDZD2 in cell lysates and concentrated conditioned media of LNCaP (lane 1), DU145 (lane 2), PC-3 (lane 3), 22Rv1 (lane 4), and RWPE-1 (lane 5) cells were detected by immunoblotting, using rabbit anti-PDZD2 antiserum (1:10,000 dilution). B, Detection of sPDZD2 secretion using rabbit anti-PDZD2 antiserum in the concentrated conditioned media harvested from DU145, PC-3, 22Rv1, and RWPE-1 cells treated with (+) or without (−) 10 μM Z-DEVD-FMK for 48 h. C, Detection of PDZD2 expression using rabbit anti-PDZD2 antiserum in lysates of DU145, PC-3, 22Rv1, and RWPE-1 cells treated with (+) or without (−) 10 μM Z-DEVD-FMK for 48 h. RWPE-1 (D), DU145 (E), PC-3 (F), and 22Rv1 (G) cells were treated with 10 μM Z-DEVD-FMK, 10 μM Z-FA-FMK, or vehicle for 24 and 48 h. H, DU145, PC-3, 22Rv1, and RWPE-1 cells were incubated with 10 μM Z-DEVD-FMK, 10 μM Z-FA-FMK, 10 μM Z-DEVD-FMK plus 10^{-8} M sPDZD2, or vehicle for 48 h. Cell proliferation was monitored by MTS assays. Data are shown as mean ± SE. *, $P < 0.01$ and ** $P < 0.001$, compared with control.

balt3/zee-end/zee-end/zee01106/zee2979-06a | taylormp | S=6 | 8/23/06 | 20:40 | Art: EN-06-0207 | Input-ss

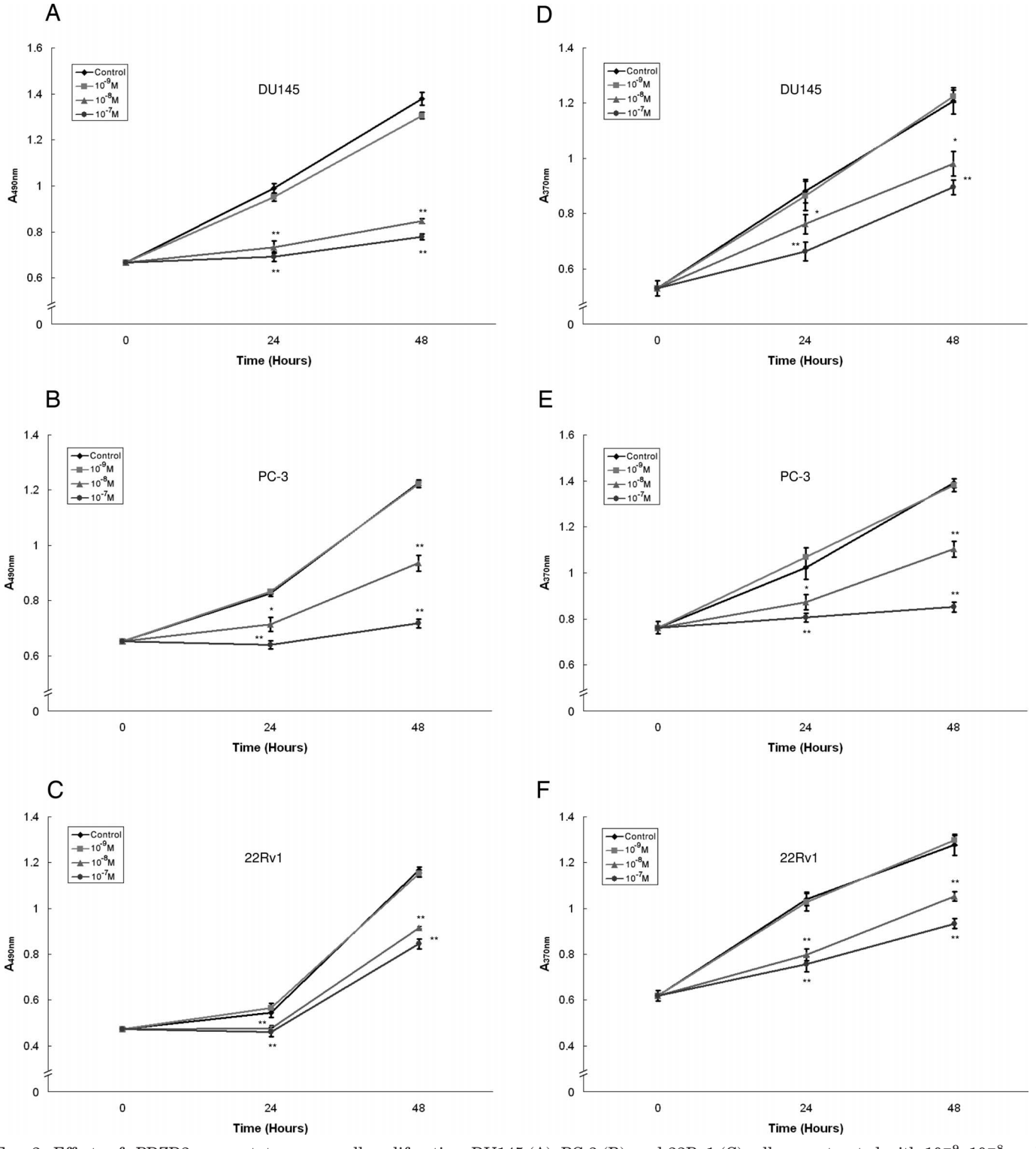

FIG. 2. Effects of sPDZD2 on prostate cancer cell proliferation. DU145 (A), PC-3 (B), and 22Rv1 (C) cells were treated with 10^{-9}, 10^{-8}, and 10^{-7} M recombinant sPDZD2 for 24 and 48 h. The effects of sPDZD2 on cell proliferation were monitored by MTS assays. The proliferation of DU145 (D), PC-3 (E), and 22Rv1 (F) cells treated with 10^{-9}, 10^{-8}, and 10^{-7} M recombinant sPDZD2 for 24 and 48 h was also monitored by cell proliferation ELISA BrdU (colorimetric) assays. Data are shown as mean ± SE. *, $P < 0.01$ and **, $P < 0.001$, compared with control.

scription induced by sPDZD2, we monitored $p21^{CIP1/WAF1}$ promoter activity in DU145 cells in response to sPDZD2 treatment using luciferase reporter assays. Treatment of DU145 cells with 10^{-8} and 10^{-7} M sPDZD2 for 24 h resulted in, respectively, 1.4- and 1.8-fold increases ($P < 0.01$) in $p21^{CIP1/WAF1}$ promoter activity. Similarly, treatment of DU145 cells with 10^{-8} and 10^{-7} M

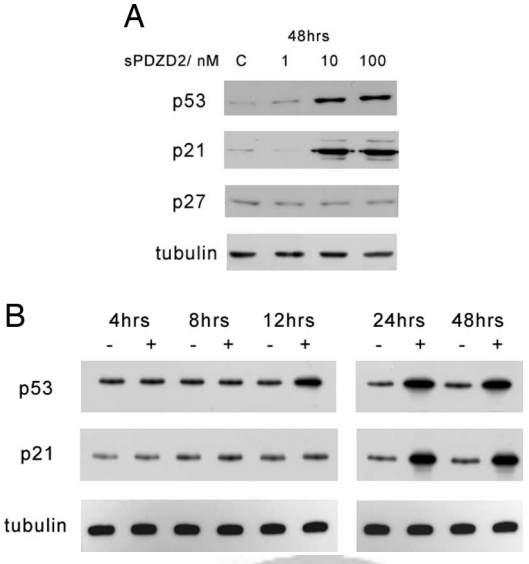

FIG. 3. Effects of sPDZD2 on $p21^{CIP1/WAF1}$, $p27^{KIP1}$, and p53 expression. A, DU145 cells were treated with 10^{-9}, 10^{-8}, and 10^{-7} M recombinant sPDZD2 for 48 h, and $p21^{CIP1/WAF1}$, $p27^{KIP1}$, and p53 levels were detected by immunoblotting. B, Time-course studies of $p21^{CIP1/WAF1}$ and p53 expression after DU145 cells were incubated with (+) or without (−) 10^{-8} M recombinant sPDZD2 for various time intervals.

sPDZD2 for 48 h resulted in 1.4- and 2.2-fold increases ($P < 0.01$) in $p21^{CIP1/WAF1}$ promoter activity, respectively (Fig. 5A). No significant changes in the promoter activity of $p27^{KIP1}$ could be detected (Fig. 5B). The $p21^{CIP1/WAF1}$ and $p27^{KIP1}$ promoter activity changes induced by sPDZD2 were in good correlation with sPDZD2-induced changes in $p21^{CIP1/WAF1}$ and $p27^{KIP1}$ mRNA levels as quantitated by RT-PCR. Treatment of DU145 cells with 10^{-8} and 10^{-7} M sPDZD2 for 24 h resulted in 2.6- and 2.9-fold increases in $p21^{CIP1/WAF1}$ mRNA levels, whereas no changes in $p27^{KIP1}$ mRNA could be detected (Fig. 5C).

Effects of sPDZD2 on cell cycle progression

The growth suppressive effects of sPDZD2 on DU145 cells were monitored by flow cytometry. Treatment of synchronized DU145 cells with 10^{-8} M sPDZD2 delayed the entry of the cells to the S phase of cell cycle. Without sPDZD2 treatment, the synchronized DU145 cells reenter into S phase by 12 h after replating, as reflected by an increase in the percentage of S phase cells from 22.1 to 38.9% (Fig. 6A). In contrast, most of the sPDZD2-treated cells remained in the G_0/G_1 phase, and no significant increase in the percentage of S phase cells was observed until 48 h after replating (Fig. 6B). Similar to DU145 cells, untreated synchronized PC-3 and 22Rv1 cells reenter into S phase by 12 h after replating, as reflected by an increase in the percentage of S phase cells from 25.4 to 34.8% and from 25.4 to 33.7%, respectively, whereas most of the sPDZD2-treated PC-3 and 22Rv1 cells remained in the G_0/G_1 phase until 48 h after replating (data not shown).

Discussion

In this communication, we demonstrated the endogenous intracellular expression of PDZD2 and extracellular secretion of its cleavage product sPDZD2 in human prostate cancer LNCaP, DU145, PC-3, and 22Rv1 cell lines as well as the immortalized RWPE-1 cells (Fig. 1A). Furthermore, the cleavage of sPDZD2 from its precursor PDZD2 in prostate cancer cells is shown to be mediated by a caspase-3-dependent mechanism, similar to that reported for the proteolytic processing of IL-16 from pro-IL-16 (19) (Fig. 1, B and C). Importantly, inhibition of endogenous sPDZD2 production and secretion by DU145, PC-3, 22Rv1, and RWPE-1 cells via the specific caspase-3 inhibitor Z-DEVD-FMK resulted in increased cell proliferation, which can be abrogated by supplementation with exogenous recombinant sPDZD2 (Figs. 1, D–H). The results suggest that endogenous sPDZD2 may exert an autocrine physiological antiproliferative action on human prostate cancer cells. Although we estimated the concentration of endogenous sPDZD2 in the conditioned cell culture media to be in the range of 10^{-10} to 10^{-11} M, it remains to be determined whether this reflects the actual concentration of sPDZD2 in human interstitial fluid or plasma. Notwithstanding this limitation of the yet-unknown physiological concentration of sPDZD2, it is noteworthy that the predicted antiproliferative actions can indeed be induced in the cancerous prostate epithelial cells by treating them with recombinant sPDZD2 (Fig. 2), which provide support for our postulation that sPDZD2 may function as an autocrine growth suppressor for human prostate cancer cells. It is also evident from our studies that sPDZD2 can suppress prostate cancer cell growth by not only antiproliferation as shown in DU145, PC-3, and 22Rv1 cells but also apoptosis induction in LNCaP cells (Fig. 4). Together with the reported up-regulation of gene and protein expression of PDZD2, also known as AIPC, in human prostate cancer tissues (12), our data indicate that sPDZD2, a proteolytic secretory product of PDZD2, may indeed play an important role in growth dysregulation in prostate cancer tumorigenesis and progression.

Flow cytometric data have indicated that antiproliferative effects of sPDZD2 on DU145, PC-3, and 22Rv1 cells are largely mediated via slowing the entry of these cancer cells into the S phase of the cell cycle (Fig. 6). In DU145 cells, we found an increase in p53 protein expression, followed by correlative increases in the gene and protein expression of $p21^{CIP1/WAF1}$, which is an important p53 transcriptional target (22) (Figs. 3 and 5). The observed slowing of DU145 cell cycle progression from G_1 to S in response to sPDZD2 can thus be adequately explained by sPDZD2-induced up-regulated gene and protein expression of $p21^{CIP1/WAF1}$, which is a well-known cyclin-dependent kinase inhibitor crucial for G_1 mitotic checkpoint regulation (23). Interestingly, the DU145 cell line, in which more than 90% of the cells show positive immunoreactivity for p53 (24), carries two mutant *p53* alleles producing $p53^{223Leu}$ and $p53^{274Phe}$, whose transactivation abilities on p53-responsive genes differ from each other (25). It has been shown that $p53^{223Leu}$ was as active as wild-type p53 in transactivation of p53-responsive genes such as $p21^{CIP1/WAF1}$, whereas $p53^{274Phe}$ has no detectable transactivation activity on those genes in a direct transactivation assay (25). Apparently sPDZD2 has the ability to activate $p53^{223Leu}$-$p21^{CIP1/WAF1}$ signaling pathway in DU145 cells to mediate its cytostatic actions observed in the present study, although the remote possibility of $p21^{CIP1/WAF1}$ activation by p53-independent mechanisms may still need to be

balt3/zee-end/zee-end/zee01106/zee2979-06a | taylormp | S=6 | 8/23/06 | 20:40 | Art: EN-06-0207 | Input-ss

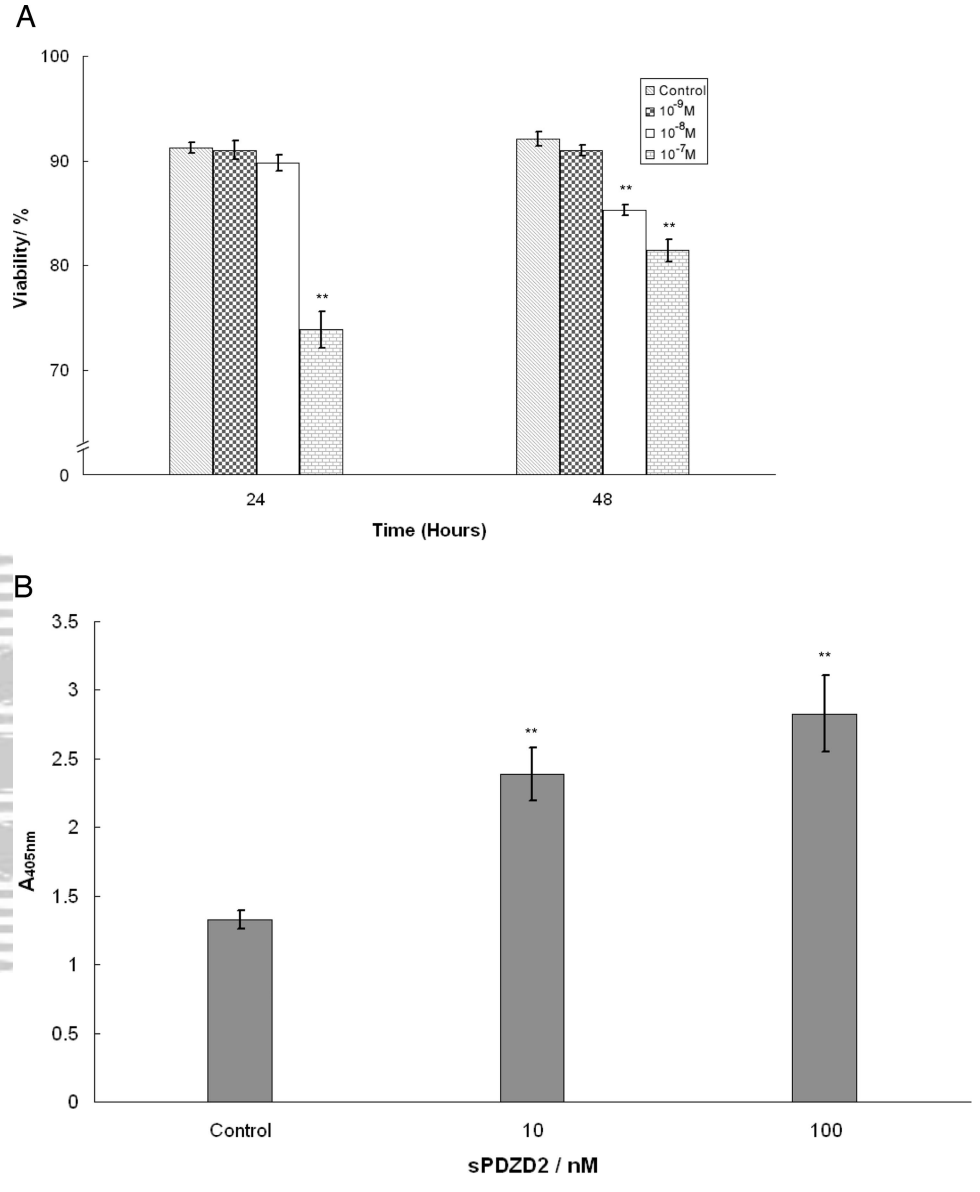

FIG. 4. Effects of sPDZD2 on LNCaP cell growth. A, LNCaP cells were treated with 10^{-9}, 10^{-8}, and 10^{-7} M recombinant sPDZD2 for 24 and 48 h. The effects of sPDZD2 on cell viability were monitored by trypan blue dye exclusion assays. B, Cell death detection ELISA^{PLUS} assay kit (Roche) was used to determine the apoptotic effects of sPDZD2 on LNCaP cells. After treatment of the cells with 10^{-8} and 10^{-7} M recombinant sPDZD2 for 24 h, the cells were lysed and the presence of nucleosomes in the cytoplasm was detected by measuring absorbance values at 405 nm. Data are shown as mean ± SE. **, $P < 0.001$, compared with control. C, LNCaP cells were treated with 10^{-9}, 10^{-8}, and 10^{-7} M recombinant sPDZD2 for 24 and 48 h. The level of Bad and the processing of PARP were monitored by immunoblotting.

balt3/zee-end/zee-end/zee01106/zee2979-06a | taylormp | S=6 | 8/23/06 | 20:40 | Art: EN-06-0207 | Input-ss

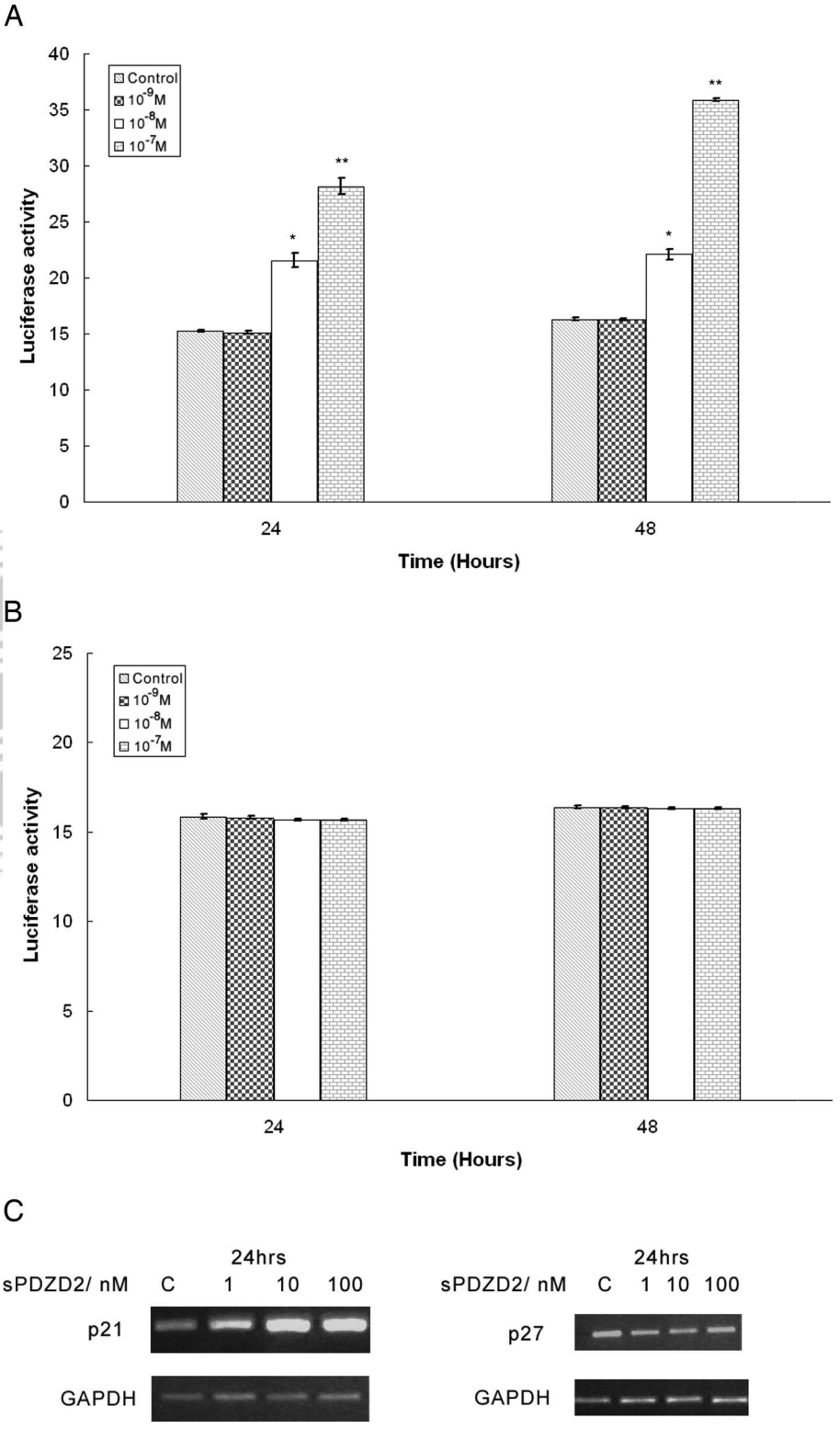

FIG. 5. Effects of sPDZD2 on $p21^{CIP1/WAF1}$ and $p27^{KIP1}$ gene transcription. The promoter activities of $p21^{CIP1/WAF1}$ (A) and $p27^{KIP1}$ (B) were monitored by luciferase reporter assays after DU145 cells were treated with 10^{-9}, 10^{-8}, and 10^{-7} M recombinant sPDZD2 for 24 and 48 h. Data are shown as mean ± SE. *, $P < 0.01$ and **, $P < 0.001$, compared with control. C, Total RNA was extracted from DU145 cells treated with or without 10^{-9}, 10^{-8}, and 10^{-7} M recombinant sPDZD2 for 24 h using TRIzol (Invitrogen) and was reversely transcribed into cDNA by using the SuperScript III first-strand synthesis system (Invitrogen). After 40 cycles of amplification by PCR, the PCR products were separated by 1.5% agarose gel. GAPDH, Glyceraldehyde-3-phosphate dehydrogenase.

considered in future studies. In an attempt to further define the mechanisms involved in p53 up-regulation and activation in DU145 cells by sPDZD2, we examined any sPDZD2-induced changes in phosphorylation at specific serine residues of p53 in DU145 cells, using a panel of antibodies against phospho-p53 (Ser6, Ser9, Ser15, Ser20, Ser37, Ser46, and Ser392). Intriguingly, we were unable to detect any significant sPDZD2-induced changes in p53 phosphorylation at the aforementioned serine residues in DU145 cells. Because active p53 is subject to a diverse array of covalent posttranslational modifications, any sPDZD2-induced changes in protein phosphorylation at sites outside those examined and in

balt3/zee-end/zee-end/zee01106/zee2979-06a | taylormp | S=6 | 8/23/06 | 20:40 | Art: EN-06-0207 | Input-ss

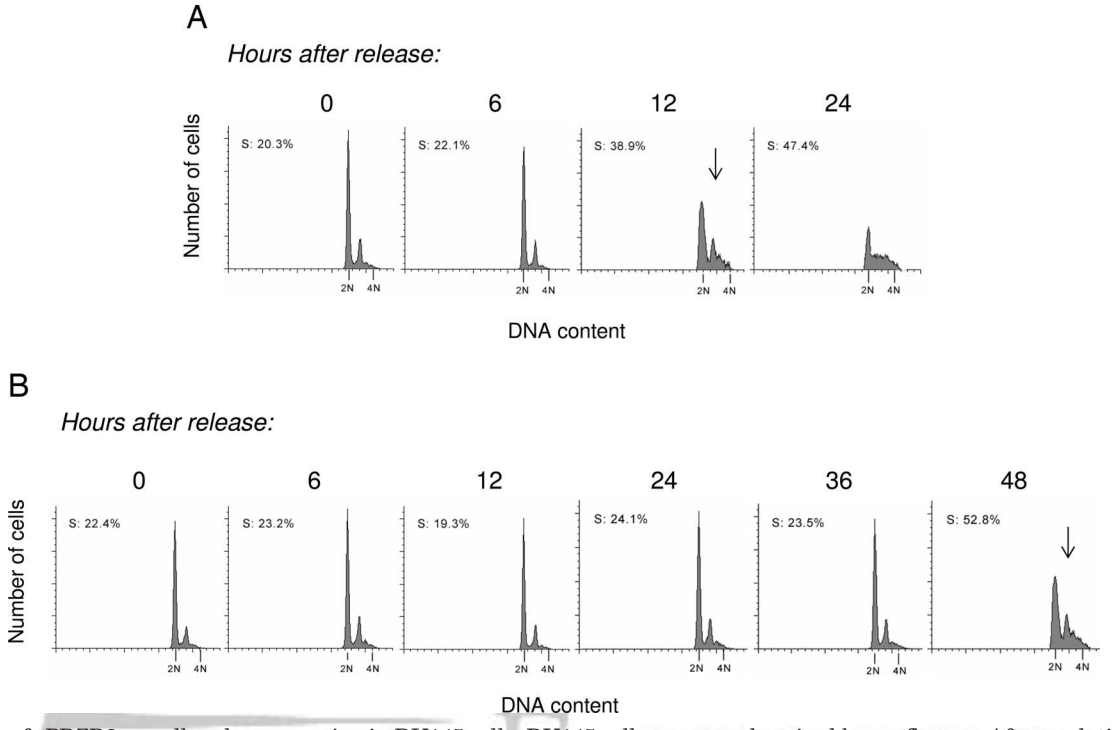

FIG. 6. Effects of sPDZD2 on cell cycle progression in DU145 cells. DU145 cells were synchronized by confluency. After replating the cells at approximately 30% confluency, in Eagle's MEM with or without 10^{-8} M recombinant sPDZD2, the cells were harvested at specific time intervals. After the cells were harvested and fixed, they were treated with RNase and propidium iodide for DNA analyses. Using the EPICS Elite ESP high-performance cell sorter (Coulter Electronics), histograms of DU145 cells treated with vehicle (A) or sPDZD2 (B) were obtained. The raw data collected were analyzed by Modfit LT (version 2.0), and *arrows* indicate increases in the percentage of S-phase cells suggesting S-phase entry.

other modifications such as acetylation, ribosylation, *O*-glycosylation, ubiquitination, and sumoylation (21) will need to be examined in future studies.

Given that p53 is an important node that integrates diverse oncogenic and DNA damage signals to mediate cytostasis and apoptosis (26), we also examined whether p53 activation is likely to be a common mechanism through which sPDZD2 induces its antiproliferative or apoptotic effects on other prostate cancer PC-3, 22Rv1, and LNCaP cells. Of note, we could not detect any expression of p53 in the PC-3 cell line, which has been shown to harbor a frameshift deletion mutation in its single *p53* allele, causing a stop signal at codon 169 of the protein (27). Moreover, sPDZD2 induced no significant changes of $p21^{CIP1/WAF1}$ and $p27^{KIP1}$ in PC-3 cells. The above findings suggested that, distinct from DU145 cells, the mechanism mediating sPDZD2-induced antiproliferation in PC-3 cells is p53 independent. Similarly, no significant changes in $p21^{CIP1/WAF1}$, $p27^{KIP1}$, and p53 were induced by sPDZD2 in the 22Rv1 cell line, which probably expresses a wild-type p53 in addition to a mutated $p53^{331Arg}$, when cultured under standard conditions (24). Clearly further studies were needed to determine the importance of p53 in the antigrowth mechanisms induced by sPDZD2 on 22Rv1 cells. Whereas sPDZD2 induced LNCaP cells to undergo apoptosis as shown by increases in Bad expression and PARP cleavage (Fig. 4C), no significant changes in total cellular p53 were observed, despite the fact that the LNCaP cell line is known to express wild-type p53 (24, 28) because its expression can be up-regulated by DNA damage signal induced by irradiation (28). Moreover, sPDZD2 did not induce, in LNCaP cells, any changes in p53 phosphorylation at Ser15, Ser20, Ser37, and Ser46, which are phosphorylation sites that are important in apoptosis control by p53 (21). These results suggest that the apoptotic effect of sPDZD2 on LNCaP cells is probably mediated through p53-independent Bad up-regulation (29).

In summary, we have obtained evidence to support the existence of PDZD2/sPDZD2-mediated autocrine growth suppressive signaling pathways in human prostate cancer cells. The p53-dependent and p53-independent mechanisms of sPDZD2 in growth inhibition of DU145, PC-3, 22Rv1, and LNCaP prostate cancer cell lines observed in our studies indicate that PDZD2/sPDZD2 signaling may use different and, perhaps, new signal transduction pathways of the intrinsic tumor suppressive network in prostate cancer in different developmental or progression stages to mediate its growth suppressor actions. Detailed characterization of these PDZD2/sPDZD2 signaling pathways and identification of the membrane receptor(s) involved may yield not only new therapeutic targets for antiprostate cancer drug discovery and development but also provide novel ways, such as harnessing therapeutically the latent tumor-suppressive potential of an endogenous autocrine signaling protein like sPDZD2, to inhibit prostate cancer growth. Besides the potential therapeutic implications mentioned above, unraveling the autocrine signaling mechanisms of PDZD2/sPDZD2 in prostate cancer growth suppression will help to increase our understanding of the physiological growth-inhibitory

networks contributed by vitamin D_3/vitamin D receptor (30) and melatonin/MT_1 receptor (31–34) signaling at the endocrine level and fatty acid metabolites/peroxisome proliferator-activated receptor-γ (35, 36) signaling at the paracrine level.

Acknowledgments

Received February 16, 2006. Accepted July 20, 2006.

Address all correspondence and requests for reprints to: Dr. Stephen Y. W. Shiu or Dr. K.-M. Yao, Department of Physiology/Biochemistry, The University of Hong Kong, Laboratory Block, Faculty of Medicine Building, 21 Sassoon Road, Hong Kong, China. E-mail: sywshiu@hkucc.hku.hk or kmyao@hkusua.hku.hk.

This work was supported by Research Grants HKU7474/04M (to K.-M.Y.), 10205056, 10205953, and HKU7580/05M and the Neuroendocrinology Research Fund (to S.Y.W.S.). C.W.T. is supported by a postgraduate studentship of The University of Hong Kong, and the data presented were derived from part of his PhD thesis work.

Disclosure statement: the authors have nothing to disclose.

References

1. **Parkin DM, Bray FI, Devesa SS** 2001 Cancer burden in the year 2000 The global picture. Eur J Cancer 37(Suppl 8):S4–S66 (Corrigendum Eur J Cancer 39:848)
2. **Miyamoto H, Messing EM, Chang C** 2004 Androgen deprivation therapy for prostate cancer: current status and future prospects. Prostate 61:332–353
3. **Kambhampati S, Ray G, Sengupta K, Reddy VP, Banerjee SK, Van Veldhuizen PJ** 2005 Growth factors involved in prostate carcinogenesis. Front Biosci 10:1355–1367
4. **Danielpour D** 2005 Functions and regulation of transforming growth factor-β (TGF-β) in the prostate. Eur J Cancer 41:846–857
5. **Karhadkar SS, Bova GS, Abdallah N, Dhara S, Gardner D, Maitra A, Isaacs JT, Berman DM, Beachy PA** 2004 Hedgehog signalling in prostate regeneration, neoplasia and metastasis. Nature 431:707–712
6. **Sanchez P, Hernandez AM, Stecca B, Kahler AJ, DeGueme AM, Barrett A, Beyna M, Datta MW, Datta S, Ruiz i Altaba A** 2004 Inhibition of prostate cancer proliferation by interference with SONIC HEDGEHOG-GLI1 signaling. Proc Natl Acad Sci USA 101:12561–12566
7. **Fan L, Pepicelli CV, Dibble CC, Catbagan W, Zarycki JL, Laciak R, Gipp J, Shaw A, Lamm ML, Munoz A, Lipinski R, Thrasher JB, Bushman W** 2004 Hedgehog signaling promotes prostate xenograft tumor growth. Endocrinology 145:3961–3970
8. **Sheng T, Li C, Zhang X, Chi S, He N, Chen K, McCormick F, Gatalica Z, Xie J** 2004 Activation of the hedgehog pathway in advanced prostate cancer. Mol Cancer 3:29
9. **Nagase T, Ishikawa K, Nakajima D, Ohira M, Seki N, Miyajima N, Tanaka A, Kotani H, Nomura N, Ohara O** 1997 Prediction of the coding sequences of unidentified human genes. VII. The complete sequences of 100 new cDNA clones from brain which can code for large proteins *in vitro*. DNA Res 4:141–150
10. **Thomas MK, Yao KM, Tenser MS, Wong GG, Habener JF** 1999 Bridge-1, a novel PDZ-domain coactivator of E2A-mediated regulation of insulin gene transcription. Mol Cell Biol 19:8492–8504
11. **Deguchi M, Iizuka T, Hata Y, Nishimura W, Hirao K, Yao I, Kawabe H, Takai Y**2000 PAPIN. A novel multiple PSD-95/Dlg-A/ZO-1 protein interacting with neural plakophilin-related armadillo repeat protein/Δ-catenin and p0071. J Biol Chem [Erratum (2000) 277:35778] 275:29875–29880
12. **Chaib H, Rubin MA, Mucci NR, Li L, Taylor JMG, Day ML, Rhim JS, Macoska JA** 2001 Activated in prostate cancer: a PDZ domain-containing protein highly expressed in human primary prostate tumors. Cancer Res 61:2390–2394
13. **Yeung ML, Tam TS, Tsang AC, Yao KM** 2003 Proteolytic cleavage of PDZD2 generates a secreted peptide containing two PDZ domains. EMBO Rep 4:412–418
14. **Fanning AS, Anderson JM** 1999 PDZ domains: fundamental building blocks in the organization of protein complexes at the plasma membrane. J Clin Invest 103:767–772
15. **Songyang Z** 1999 Recognition and regulation of primary-sequence motifs by signaling modular domains. Prog Biophys Mol Biol 71:359–372
16. **Ma RYM, Tam TSM, Suen APM, Yeung PML, Tsang SW, Chung SK, Thomas MK, Leung PS, Yao KM** 2006 Secreted PDZD2 exerts concentration-dependent effects on the proliferation of INS-1E cells. Int J Biochem Cell Biol 38:1015–1022
17. **Han S, Sidell N, Roman J** 2005 Fibronectin stimulates human lung carcinoma cell proliferation by suppressing p21 gene expression via signals involving Erk and Rho kinase. Cancer Lett 219:71–81
18. **Buchwald PC, Akerstrom G, Westin G** 2004 Reduced p18INK4c, p21CIP1/WAF1 and p27KIP1 mRNA levels in tumours of primary and secondary hyperparathyroidism. Clin Endocrinol (Oxf) 60:389–393
19. **Zhang Y, Center DM, Wu DM, Cruikshank WW, Yuan J, Andrews DW, Kornfeld H** 1998 Processing and activation of pro-interleukin-16 by caspase-3. J Biol Chem 273:1144–1149
20. **Fridman JS, Lowe SW** 2003 Control of apoptosis by p53. Oncogene 22:9030–9040
21. **Bode AM, Dong Z** 2004 Post-translational modification of p53 in tumorigenesis. Nat Rev Cancer 4:793–805
22. **el-Deiry WS, Tokino T, Velculescu VE, Levy DB, Parsons R, Trent JM, Lin D, Mercer WE, Kinzler KW, Vogelstein B** 1993 WAF1, a potential mediator of p53 tumor suppression. Cell 75:817–825
23. **Nakayama K, Nakayama K** 1998 Cip/Kip cyclin-dependent kinase inhibitors: brakes of the cell cycle engine during development. Bioessays 20:1020–1029
24. **van Bokhoven A, Varella-Garcia M, Korch C, Johannes WU, Smith EE, Miller HL, Nordeen SK, Miller GJ, Lucia MS** 2003 Molecular characterization of human prostate carcinoma cell lines. Prostate 57:205–225
25. **Gurova KV, Rokhlin OW, Budanov AV, Burdelya LG, Chumakov PM, Cohen MB, Gudkov AV** 2003 Cooperation of two mutant p53 alleles contributes to Fas resistance of prostate carcinoma cells. Cancer Res 63:2905–2912
26. **Massague J** 2004 G_1 cell-cycle control and cancer. Nature 432:298–306
27. **Carroll AG, Voeller HJ, Sugars L, Gelmann EP** 1993 p53 oncogene mutations in three human prostate cancer cell lines. Prostate 23:123–134
28. **Bohnke A, Westphal F, Schmidt A, El-Awady RA, Dahm-Daphi J** 2004 Role of p53 mutations, protein function and DNA damage for the radiosensitivity of human tumour cells. Int J Radiat Biol 80:53–63
29. **Butt AJ, Firth SM, King MA, Baxter RC** 2000 Insulin-like growth factor-binding protein-3 modulates expression of Bax and Bcl-2 and potentiates p53-independent radiation-induced apoptosis in human breast cancer cells. J Biol Chem 275:39174–39181
30. **Krishnan AV, Peehl DM, Feldman D** 2003 Inhibition of prostate cancer growth by vitamin D: regulation of target gene expression. J Cell Biochem 88:363–371
31. **Xi SC, Tam PC, Brown GM, Pang SF, Shiu SYW** 2000 Potential involvement of mt_1 receptor and attenuated sex steroid-induced calcium influx in the direct anti-proliferative action of melatonin on androgen-responsive LNCaP human prostate cancer cells. J Pineal Res 29:172–183
32. **Xi SC, Siu SWF, Fong SW, Shiu SYW** 2001 Inhibition of androgen-sensitive LNCaP prostate cancer growth *in vivo* by melatonin: association of anti-proliferative action of the pineal hormone with mt_1 receptor protein expression. Prostate 46:52–61
33. **Siu SWF, Lau KW, Tam PC, Shiu SYW** 2002 Melatonin and prostate cancer cell proliferation: interplay with castration, epidermal growth factor, and androgen sensitivity. Prostate [Erratum (2000) 52:252] 52:106–122
34. **Shiu SYW, Law IC, Lau KW, Tam PC, Yip AWC, Ng WT** 2003 Melatonin slowed the early biochemical progression of hormone-refractory prostate cancer in a patient whose prostate tumor tissue expressed MT_1 receptor subtype. J Pineal Res 35:177–182
35. **Schopfer FJ, Lin Y, Baker PR, Cui T, Garcia-Barrio M, Zhang J, Chen K, Chen YE, Freeman BA** 2005 Nitrolinoleic acid: an endogenous peroxisome proliferator-activated receptor γ ligand. Proc Natl Acad Sci USA 102:2340–2345
36. **Kim J, Yang P, Suraokar M, Sabichi AL, Llansa ND, Mendoza G, Subbarayan V, Logothetis CJ, Newman RA, Lippman SM, Menter DG** 2005 Suppression of prostate tumor cell growth by stromal cell prostaglandin D synthase-derived products. Cancer Res 65:6189–6198

AUTHOR QUERIES

AUTHOR PLEASE ANSWER ALL QUERIES **1**

A—Please verify location of American Type Culture Collection, Life Technologies, and New England Biolabs.

B—Please confirm definition of MTS and BrdU.

C—Please verify location of BD Biosciences, Promega, and Roche.

D—Please define TBS-T.

E—Please verify locations of Millipore, Zymed, and Amersham Biosciences.

F—Please verify location of EG&G Berthold.

G—Please verify location of Invitrogen.

H—Please verify dNTP as written out.

I—Please verify location of Coulter Electronics and Verity Software.